RAPID COMMUNICATIONS

PHYSICAL REVIEW B VOLUME 43, NUMBER 13 1 MAY 1991

Incident-beam enhancements of Auger electron scattering

Y. U. Idzerda and G. A. Prinz
Naval Research Laboratory, Washington, D.C. 20375-5000
(Received 17 January 1991)

The role of scattering of the incident excitation electrons is examined by use of judiciously chosen scattering geometries that allow for the experimental separation of incident-beam effects and Auger-electron-scattering effects. The scattering of 4-keV incident electrons can result in variations greater than 25% of the Auger electron intensity for scattering from bcc Fe(001). A simple procedure for detecting the presence of incident-beam effects in other systems is given.

The structural determination of overlayers and ultrathin films by angle-resolved electron emission and subsequent electron scattering is well established,[1,2] demonstrating good agreement with other structural probes. Often, the scattering of electrons produced by photoelectron emission from photon absorption and Auger electron emission from electron-beam excitation are analyzed in similar manners,[3-5] even though the physical mechanisms generating the electron emission are different. This similarity in treatments is believed to be valid if the angular character of the Auger emission is modeled correctly and if there are no significant variations in the Auger intensity from the transmission of the incident excitation electron beam (incident-beam channeling effects). Under these conditions, the extensive theoretical methods developed for x-ray photoelectron scattering[1,2,6] can be directly applied to understanding Auger-electron-scattering data.

The role of the transmission of the incident excitation electron beam and the resulting variations of Auger intensity have been addressed experimentally with conflicting results. Earlier works found that Auger electron intensity changes did show some dependence on incident-beam direction. It was found that the 2π-angle-integrated Auger peak intensity for Al showed 30% variations in intensity.[7] Similar results were found for As(0001) surfaces.[8] Smaller modulations were measured for Cu Auger electrons using a cylindrical-mirror analyzer.[9] These studies concluded that there is a significant dependence of the integrated Auger intensity on the incident-beam direction. The opposite conclusion was reached in a recent study which addressed precisely the role of incident-beam effects in the angle-resolved Auger electron spectra.[10] Using a fully angular-resolved electron detector but limited to polar angle scans using only two distinct angles of incidence for the electron source (20° and 90° from the θ-rotation axis) it was concluded that incident-beam channeling was not a major contributing factor to the Auger electron intensity modulations. These conclusions were also obtained in an investigation[11] of incident-beam effects for medium-energy electron diffraction, a technique where structural information is extracted from the angular profiles of elastically scattered electrons of 1–5 keV energy.[12] On the strength of these more recent studies, theoretical treatments have omitted incident-beam scattering in modeling of electron-induced Auger electron emission and the subsequent emitted electron scattering.[3-5] In this paper, the role of scattering of the incident excitation electrons has been reexamined for a judiciously chosen scattering geometry which unambiguously measures the contribution of incident-beam effects on the resulting angle-resolved Auger spectra. Our results find these effects to be too large to be ignored, bringing into question the assumptions underlying the theoretical methods currently used for understanding Auger electron scattering.

The scattering geometry for these experiments has been carefully chosen in an attempt to investigate only the effect of forward-scattering enhancements of the incident electrons on intensity variations in Auger electron emission (see Fig. 1). Three types of measurements were taken in this study; a polar scan, a normal-emission azimu-

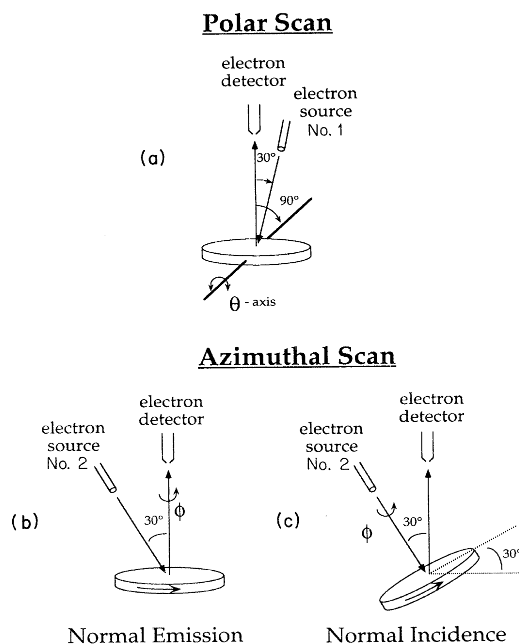

FIG. 1. Experimental scattering geometries. (a) Polar scan configuration (using electron source No. 1), source, detector, and θ-rotation axes are in the same plane. (b) Normal-emission azimuthal scan configuration (using electron source No. 2). (c) Normal-incidence azimuthal scan configuration.

Work of the U.S. Government
Not Subject to U.S. Copyright

thal scan, and a normal-incidence azimuthal scan. It is the second and third measurement which allow for the separation and identification of incident-beam effects. The first scattering geometry, shown in Fig. 1(a), allows for the acquisition of the θ dependence of the Auger electron intensity (polar scans) to determine the quality of the crystalline structure of the sample. In this configuration, the electron source (labeled No. 1), the electron detector, and the θ-rotation axis are all in the same plane.

The second type of measurement allows for the acquisition of normal-emission azimuthal scans. In this scattering geometry, shown in Fig. 1(b), the electron source (labeled No. 2) is directed perpendicular to the θ-rotation axis. With the detector axis normal to the face of the sample ($\theta=0°$), an azimuthal rotation of the sample does not alter the Auger emission geometry. In other words, because of the cylindrical symmetry of the sample-detector geometry, the flux of Auger electrons measured perpendicular to the film plane is insensitive to the azimuthal position of the sample (for a symmetric instrumental aperture). Therefore, any observed intensity variation of the normal-emission Auger electrons due to azimuthal rotation is an indication that incident-beam effects are present. The azimuthal sample rotation effectively sweeps the incident electron direction in a cone of 30° centered on the detector axis.

In Fig. 1(c) we show the third scattering geometry which exchanges the incident-beam direction and the electron detector direction, allowing for the acquisition of normal-incidence azimuthal scans. This is accomplished by tilting the sample ($\theta=30°$) so that the electron beam is now incident normal to the sample and the detector is positioned 30° from the sample normal (electron source No. 2 is again used). In this configuration, incident-beam effects are minimized. An azimuthal rotation of the crystal (azimuthal scan) will not change the direction of incidence of the electron beam within the crystal and will result in no variation of the Auger emission intensity due to the incident beam. (Incident-beam forward-scattering enhancements may still be present, but will not vary with azimuthal rotation.) In this geometry, variations in the measured Auger electron intensity are due only to scattering of the emitted Auger electron on its way to the detector. The important point is that using these last two configurations, the role of scattering of the incident electron and scattering of the emitted Auger electron can be separately quantified in an unambiguous manner.

For these experiments, the sample is a 100-Å, single-crystal, bcc Fe(001) film epitaxially deposited on GaAs(001). Details of the film growth have been described elsewhere.[13] The incident-beam energies are 4 keV at a 5-μA emission current. The intensity of the Fe *LMM* Auger transition at 965 eV is monitored using a Vacuum Science Workshop 100-mm hemispherical electron analyzer with a variable acceptance angle. In these experiments an acceptance angle of $\pm 6°$ was used except as indicated (for comparison of electron-scattering structures using different acceptance angles). Under these conditions, complete polar and azimuthal scans of the Auger intensity are taken in 20–30 min. The apparatus is contained in a cryogenic-pumped, ion-pumped, and titanium-sublimation-pumped UHV system operated at 1×10^{-10} Torr except during Fe deposition where the pressure was 4×10^{-10} Torr. The film quality was measured by Auger electron spectroscopy and by reflection high-energy electron diffraction (RHEED) during the film growth and showed a contaminant-free ($<5\%$) film with a strong bcc structure, as has been previously observed.[13] The film thickness was measured by x-ray fluorescence after the samples were removed from the UHV chamber.

Additional structural characterization is obtained from the two polar scans of the angle-resolved Auger electron diffraction pattern of the bcc Fe(001) surface taken along the ⟨110⟩ and ⟨100⟩ axes. These scans are acquired using the first electron source position [labeled No. 1 in Fig. 1(a)] which is in the plane of the detector axis and the θ axis. The polar scans are for the peak-to-peak derivative Auger spectra and are normalized to unity intensity after a slight linear background has been removed. No additional corrections due to the instrumental response have been made to the data. The polar scan for the bcc Fe(001) surface taken along the ⟨110⟩ direction is shown in Fig. 2. The major peaks at 0°, $\pm 35°$, and $\pm 54.7°$ for the scans along the ⟨110⟩ axis are due to the forward scattering along the ⟨001⟩, ⟨112⟩, and ⟨111⟩ directions, respectively. These scans taken along the ⟨100⟩ and ⟨110⟩ directions correspond closely to a bcc structure[14] and demonstrate that the films are highly crystalline.

To better understand the basis for the intensity variations in the normal-emission and normal-incidence Auger emission plots, two different methods were used to acquire the Fe Auger intensity spectra. First, the Auger peak intensity and secondary electron background intensity were obtained by electron counting and, second, the derivative Auger spectra was measured by impressing a 6-V *p-p* sinusoidal signal on the sample potential for lock-in methods. The lock-in method was used for greatly improved signal-to-noise ratios and is the typical method which is standardly used for measuring Auger intensities.

In separately measuring the absolute Auger peak intensity and the secondary electron background intensity, we can normalize the Auger peak height to the background level. The secondary electron background level at ener-

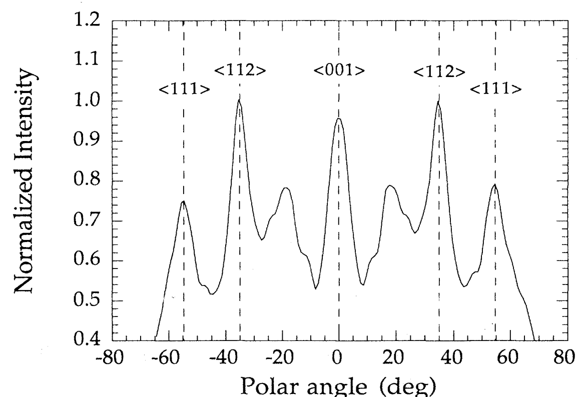

FIG. 2. Polar scan of bcc Fe(001) taken along ⟨110⟩ axis. Dashed lines show positions of major crystalline directions.

gies just above the Auger electron energy should be proportional to the incident flux of electrons within the probed sample volume.[15] Normalization of the Auger peak intensity with the background intensity will eliminate variations in the flux of quasielastic electrons within the probed region. This variation can come from changes in the incident electron flux or in changes in the direction-dependent reflection and transmission coefficients for the surface. In this experiment variations in incident flux are below 1% (as demonstrated in Fig. 5). On the other hand, various investigators have found that the transmission and reflection of high-energy (1–10 keV) electrons is strongly directional dependent. The total quasielastic yield for scattering from Al varies with the direction of incidence by up to 50%.[7] It is possible that the variations in the measured Auger intensities with the direction of incidence of the excitation beam may be due to this fluctuation in the number of excitation electrons in the probed region. In fact, the disagreement in the earlier sets of experiments of incident-beam effects (Refs. 7–9 and Refs. 10 and 11) might be an artifact of the differences in normalization procedure from this process. (References 10 and 11 were normalized to the background level.[16])

The data for the normal-emission configuration using both acquisition schemes are shown in Fig. 3. The data have been normalized to unity intensity after a linear background has been removed. To illustrate the detail, only the region between $\pm 55°$ is shown . The remaining data are highly symmetric with a fourfold symmetry which is reflective of the symmetry of the (100) surface. The major peaks are indexed to the nearest crystalline axis. It is clear from these spectra that incident-beam channeling effects are present, accounting for variations of 20%. In addition, the derivative Auger intensity and the normalized-to-background absolute Auger intensity are extremely similar in shape but with noticeable differences in intensities. The magnitude of the variations is larger in the derivative Auger spectra (where no normalization to changes in the incident flux is performed) than in the normalized-to-background peak Auger spectra. This observation is clear evidence that the number of excitation electrons within the probed sample region does vary and is dependent on the incident-beam direction, but this is not the entire source of the intensity change. Some variation of the excitation flux is occurring concurrently with the incident-beam channeling.

It is interesting to compare the spectrum for normal emission with the spectrum for normal incidence shown in Fig. 4. Again, the derivative Auger intensity and the normalized-to-background absolute Auger intensity are shown for a data range of only $\pm 55°$ for clarity. (These data have been normalized to unity intensity after subtraction of a linear background and are also fourfold symmetric.) In this case, the two spectra are the same in shape and in intensity. This is not surprising because in this configuration no variation in the incident-beam direction, and therefore the excitation flux within the sample, occurs. The indexing of the major peaks is the same as in Fig. 3. The crystalline axes chosen for indexing these features represent the nearest major peaks of the angle-resolved polar scan spectra collected at $\phi = 0°$ (along $\langle 110 \rangle$) and $\phi = 45°$ (along $\langle 100 \rangle$). None of the peaks in the polar scans are a maximum at $\theta = 30°$. The $\langle 112 \rangle$ axis occurs at $\theta = 35.3°$ and the $\langle 102 \rangle$ and $\langle 012 \rangle$ axes occur at $\theta = 26.6°$. Changing the incident-beam direction to these other polar values enhances the incident-beam effects even further.

The similar location of the major peaks for the normal-incidence and normal-emission spectra strongly suggests that the same forward-scattering enhancement mechanism which is responsible for the features in the normal-incidence Auger emission spectra is also responsible for the normal-emission Auger spectra. The differences in the spectra (location of the smaller peaks) can be related to the different energies of the scattering electron. In the normal-emission geometry, the 4-keV incident electrons are the electrons which are scattered, whereas in the

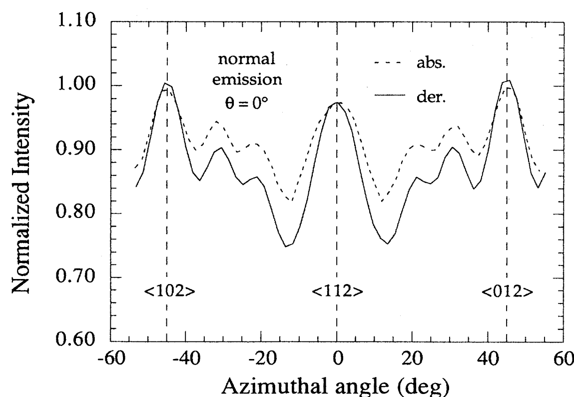

FIG. 3. Normal-emission Auger azimuthal scans for bcc Fe(001). Solid line is peak-to-peak derivative intensity. Dashed line is the absolute peak-to-background height, normalized to the secondary background level measured at an energy above the Auger electron energy. Also shown are the azimuthal positions of nearby crystalline directions.

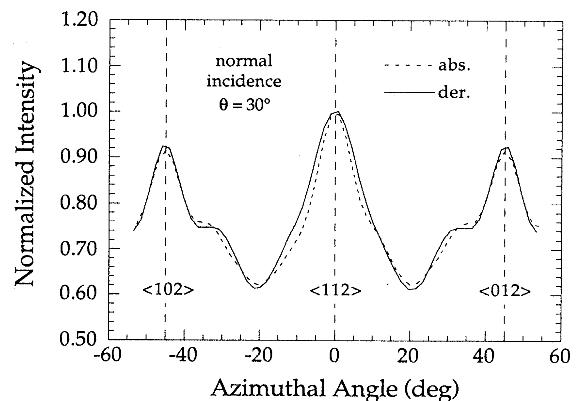

FIG. 4. Normal-incidence Auger azimuthal scans for bcc Fe(001). Solid line is peak-to-peak derivative intensity. Dashed line is the absolute peak-to-background height, normalized to the secondary background level measured at an energy above the Auger electron energy. Also shown are the azimuthal positions of nearby crystalline directions.

normal-incidence spectra it is the scattering of the ~1-keV Auger electrons which occurs. The position of the forward-scattering peaks are independent of the electron energy (for energies above 500 eV), but the position of the smaller features (whose presence is due to higher-order diffraction effects) are energy dependent.

Another possible mechanism for these variations of the observed intensity modulations (other than the mechanism described above) is an asymmetric instrument response due to asymmetric acceptance apertures, stray fields, charging, etc. This can be experimentally checked in two ways. First, the acceptance angle can be changed electronically. The resulting Auger emission spectra for a $\pm 4°$ acceptance angle are similar to that shown for a $\pm 6°$ acceptance angle, with equivalent positioning of the major peaks. Second, a polycrystalline Fe film can be deposited on the GaAs surface by depositing the Fe at a high rate on a substrate held at room temperature. Under these conditions, the RHEED shows polycrystalline rings and the polar angle-resolved Auger spectra (collected under the same conditions as Fig. 2) are essentially flat and featureless. The polycrystalline nature of the films results in no coherent forward-scattering features. The normalized azimuthal scans for both the normal-incidence and normal-emission geometries, shown in Fig. 5, also appear featureless. The uniformity of these spectra show that not only is the crystallinity of the sample essential for the formation of the Auger intensity enhancements for both the normal-incidence and normal-emission geometries, but also that the instrument response is extremely symmetric and the emission of the electron source is very constant (fluctuations less than 1%).

It is straightforward to conclude that incident-beam effects (incident-beam channeling) are present with significant intensities in electron-induced Auger emission and probably also present in medium-energy electron diffraction. Furthermore, to accurately account for these effects, theoretical treatments must incorporate the incident-beam scattering, or experimental geometries must be chosen to minimize their importance. A simple test for the presence of incident-beam effects can be performed in any system with azimuthal rotation and normal-emission capabilities.

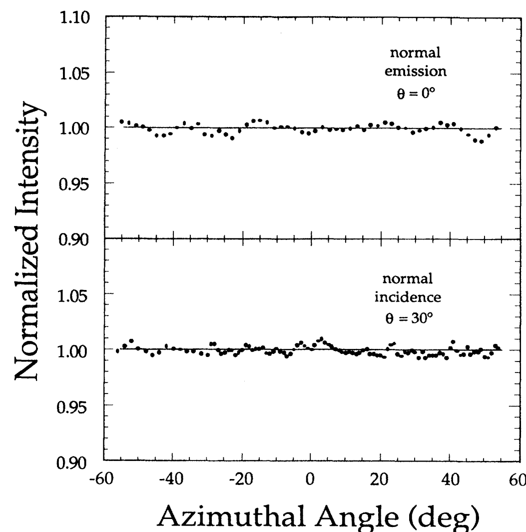

FIG. 5. Normal-emission and normal-incidence Auger azimuthal scan for polycrystalline Fe. The scans are featureless.

This work is supported by the Office of Naval Research.

[1]C. S. Fadley, in *Synchrotron Radiation Research: Advances in Surface Science*, edited by R. Z. Bachrach (Plenum, New York, 1990).

[2]C. S. Fadley, in *Progress in Surface Science*, edited by S. G. Davison (Pergamon, New York, 1984).

[3]W. F. Egelhoff, Jr., Phys. Rev. Lett. **59**, 559 (1987).

[4]S. A. Chambers, S. B. Anderson, and J. H. Weaver, Phys. Rev. B **32**, 4872 (1985).

[5]S. A. Chambers, H. W. Chen, I. M. Vitomirov, S. B. Anderson, and J. H. Weaver, Phys. Rev. B **33**, 1810 (1986).

[6]M. L. Xu and M. A. van Hove, Surf. Sci. **207**, 215 (1989).

[7]G. Allié, E. Elanc, D. Dufayard, and R. M. Stern, Surf. Sci. **46**, 188 (1974).

[8]W. P. Ellis, Surf. Sci. **41**, 125 (1974).

[9]A. F. Armitage, D. P. Woodruff, and P. D. Johnson, Surf. Sci. **100**, L483 (1980).

[10]S. A. Chambers, H. W. Chen, S. B. Anderson, and J. H. Weaver, Phys. Rev. B **34**, 3055 (1986).

[11]S. A. Chambers, I. M. Vitomirov, and J. H. Weaver, Phys. Rev. B **36**, 3007 (1987).

[12]S. A. Chambers, I. M. Vitomirov, S. B. Anderson, and J. H. Weaver, Phys. Rev. B **35**, 2490 (1987).

[13]G. A. Prinz and J. J. Krebs, Appl. Phys. Lett. **39**, 397 (1981).

[14]H. Li and B. P. Tonner, Phys. Rev. B **37**, 3959 (1988).

[15]This relies on low backgrounds due to the electronics, etc. In these measurements this background level is $<1\%$ of the secondary electron background level.

[16]S. A. Chambers (private communication). Integrated Auger peak area normalized to secondary-electron background. Procedure given in S. A. Chambers, G. A. Howell, T. R. Greenlee, and J. H. Weaver, Phys. Rev. B **31**, 6402 (1985).